

Full-waveform inversion with Hussar dataset and some synthetic examples

Wenyong Pan*, Kris Innanen and Gary Margrave

wpan@ucalgary.ca

FWI with Hussar dataset



Figure 1. The 4.5 km Hussar seismic line is shown together with the locations of 5 wells with good logging suites, shot point locations, and the location of the recorders.

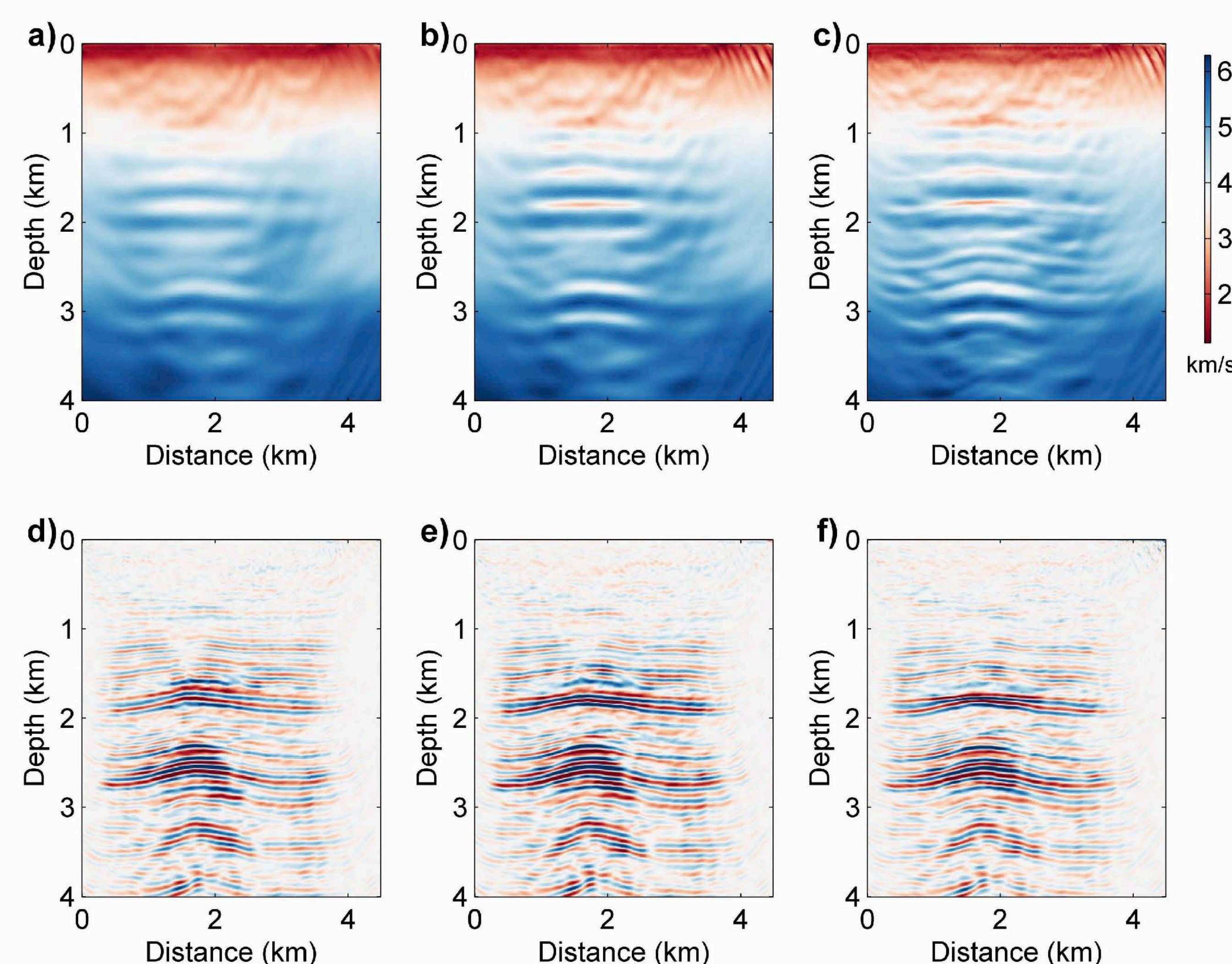


Figure 2. (a), (b) and (c) show the inversion results at 4th, 6th and 10th iterations. (d), (e) and (f) show the reverse time migration images using the corresponding inverted models

Source-independent Hessian-free Gauss-Newton FWI

The estimation of source wavelet is important for successful implementation of full-waveform inversion (FWI). Many FWI algorithms estimate the source signature iteratively in the inversion process. In this paper, a source-independent method is adopted with a data calibration process. Furthermore, the gradient-based methods for FWI suffer from slow local convergence rate. A Hessian-free (HF) Gauss-Newton method is implemented in this research by solving the Newton system with a conjugate-gradient (CG) method. With the source-independent strategy, the Gauss-Newton Hessian is also modified. We demonstrate with numerical examples that the HF Gauss-Newton method with the modified Hessian can improve the convergence rate and reduce the computational burden.

The FWI misfit function with source weight is expressed as:

$$\tilde{\Phi}(\mathbf{m}, \mathbf{s}) = \frac{1}{2} \sum_{\mathbf{x}_s} \sum_{\mathbf{x}_g} \sum_{\omega} \|\mathbf{d}_{\text{obs}}(\mathbf{x}_s, \mathbf{x}_g, \omega) - \mathbf{s}(\mathbf{x}_s, \omega) \mathbf{d}_{\text{syn}}(\mathbf{m}, \mathbf{x}_s, \mathbf{x}_g, \omega)\|^2$$

where the source weight is obtained as:

$$\mathbf{s}(\mathbf{x}_s, \omega) = \frac{\sum_{\mathbf{x}_g} \mathbf{d}_{\text{obs}}(\mathbf{x}_s, \mathbf{x}_g, \omega) \mathbf{d}_{\text{syn}}^*(\mathbf{x}_s, \mathbf{x}_g, \omega)}{\sum_{\mathbf{x}_g} \mathbf{d}_{\text{syn}}(\mathbf{x}_s, \mathbf{x}_g, \omega) \mathbf{d}_{\text{syn}}^*(\mathbf{x}_s, \mathbf{x}_g, \omega)}$$

The Jacobian matrix is expressed as:

$$\tilde{\mathbf{J}}(\mathbf{x}_s, \mathbf{x}_g, \omega) = \mathbf{s}(\mathbf{x}_s, \omega) \frac{\partial \mathbf{d}_{\text{syn}}(\mathbf{x}_s, \mathbf{x}_g, \omega)}{\partial \mathbf{m}} + \frac{\partial \mathbf{s}}{\partial \mathbf{m}} \mathbf{d}_{\text{syn}}(\mathbf{x}_s, \mathbf{x}_g, \omega)$$

The gradient and Hessian can be written as:

$$\mathbf{g} = \tilde{\mathbf{J}}^* \Delta \mathbf{d}, \tilde{\mathbf{H}}_a = \tilde{\mathbf{J}}^* \tilde{\mathbf{J}}$$

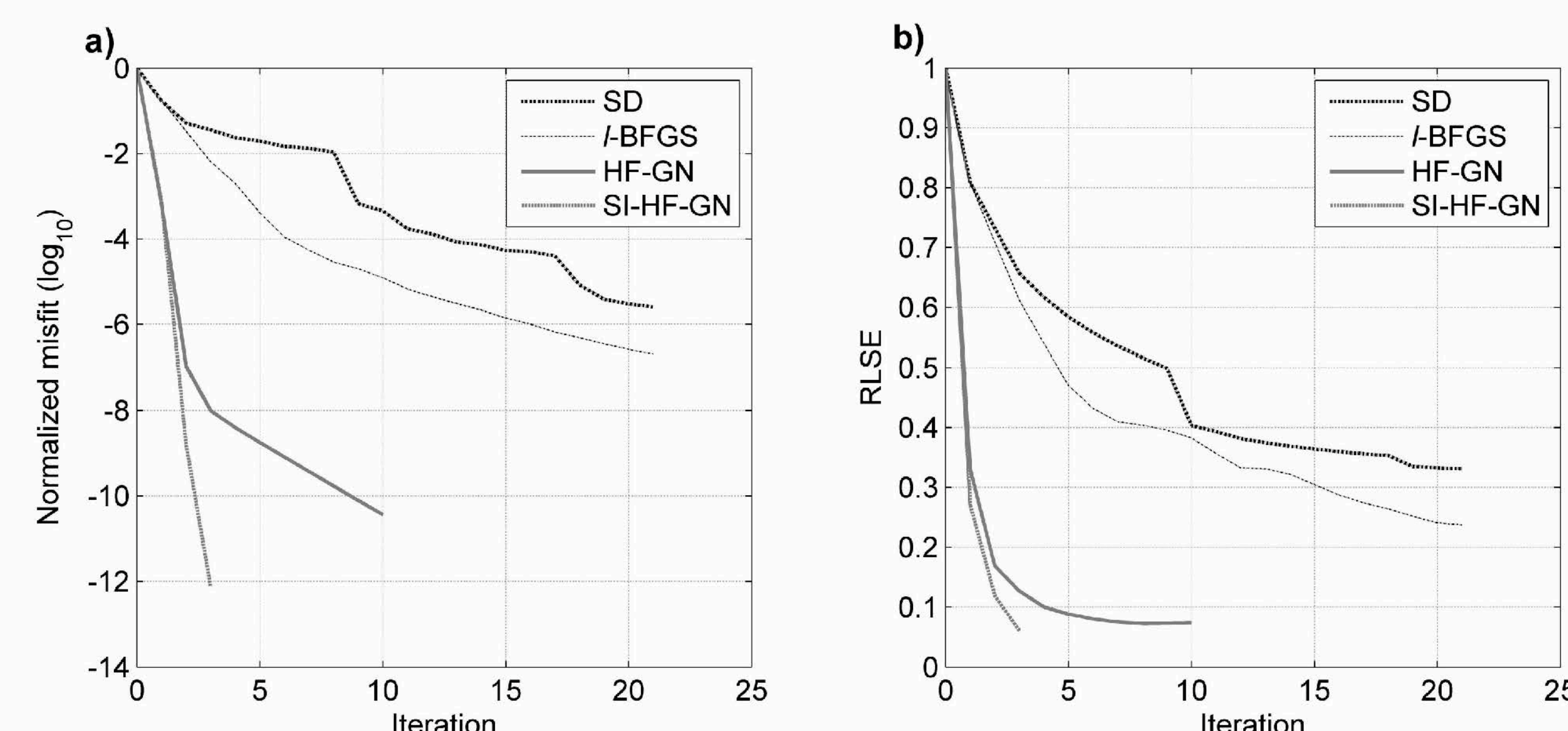


Figure 3. The convergence history of different methods.

FWI in the frequency-ray parameter domain

Forward modelling in frequency-ray parameter domain:

$$\mathbf{L}(\mathbf{x}, \omega) \tilde{\mathbf{u}}(\mathbf{x}, p, \omega) = - \sum_{\mathbf{x}_s} \exp(i\omega p(\mathbf{x}_s - \hat{\mathbf{x}}_s)) f_s(\omega) \delta(\mathbf{x} - \mathbf{x}_s)$$

The slant gradient with ray parameter p is expressed as:

$$\tilde{\mathbf{g}}(\mathbf{x}, p) = \sum_{\mathbf{x}_s} \sum_{\mathbf{x}_g} \sum_{\omega} \Re(\omega^2 f_s(\omega) G(\mathbf{x}, \mathbf{x}_s, \omega) G^*(\mathbf{x}, \mathbf{x}_g, \omega) \Delta \mathbf{d}^*(\mathbf{x}_g, \mathbf{x}'_s, \omega) \times A^2(\omega) \exp(i\omega p(\mathbf{x}_s - \mathbf{x}'_s)))$$

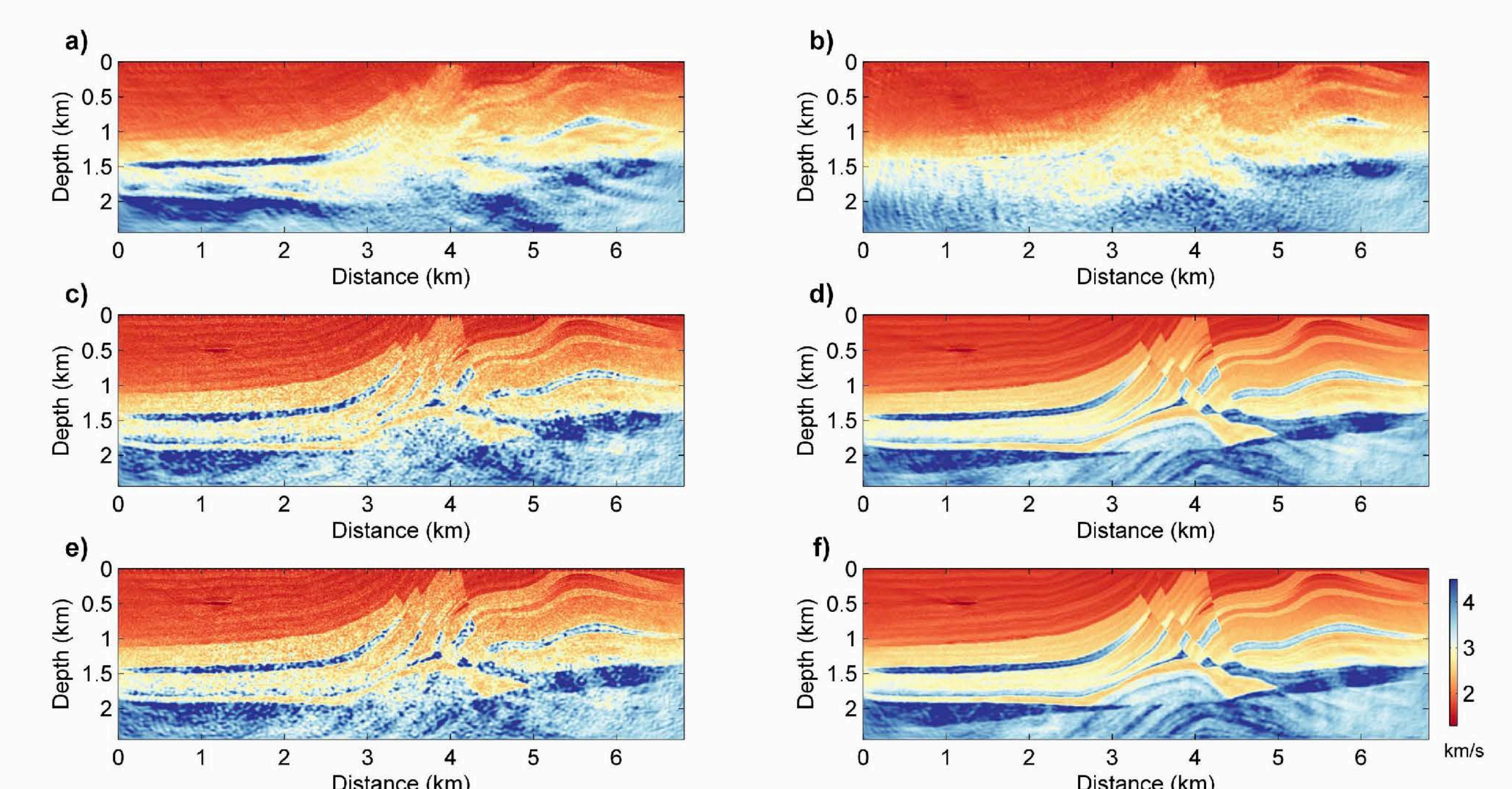


Figure 4. (a) Mono-frequency slant update with $p = -0.01$ s/km; (b) Mono-frequency slant update with $p = -0.03$ s/km; (c) Mono-frequency random slant update; (d) Partial overlap-frequency random slant update ($\epsilon = 0.4862$); (e) Mono-frequency sequential slant update; (f) Partial overlap-frequency sequential slant update ($\epsilon = 0.4596$).

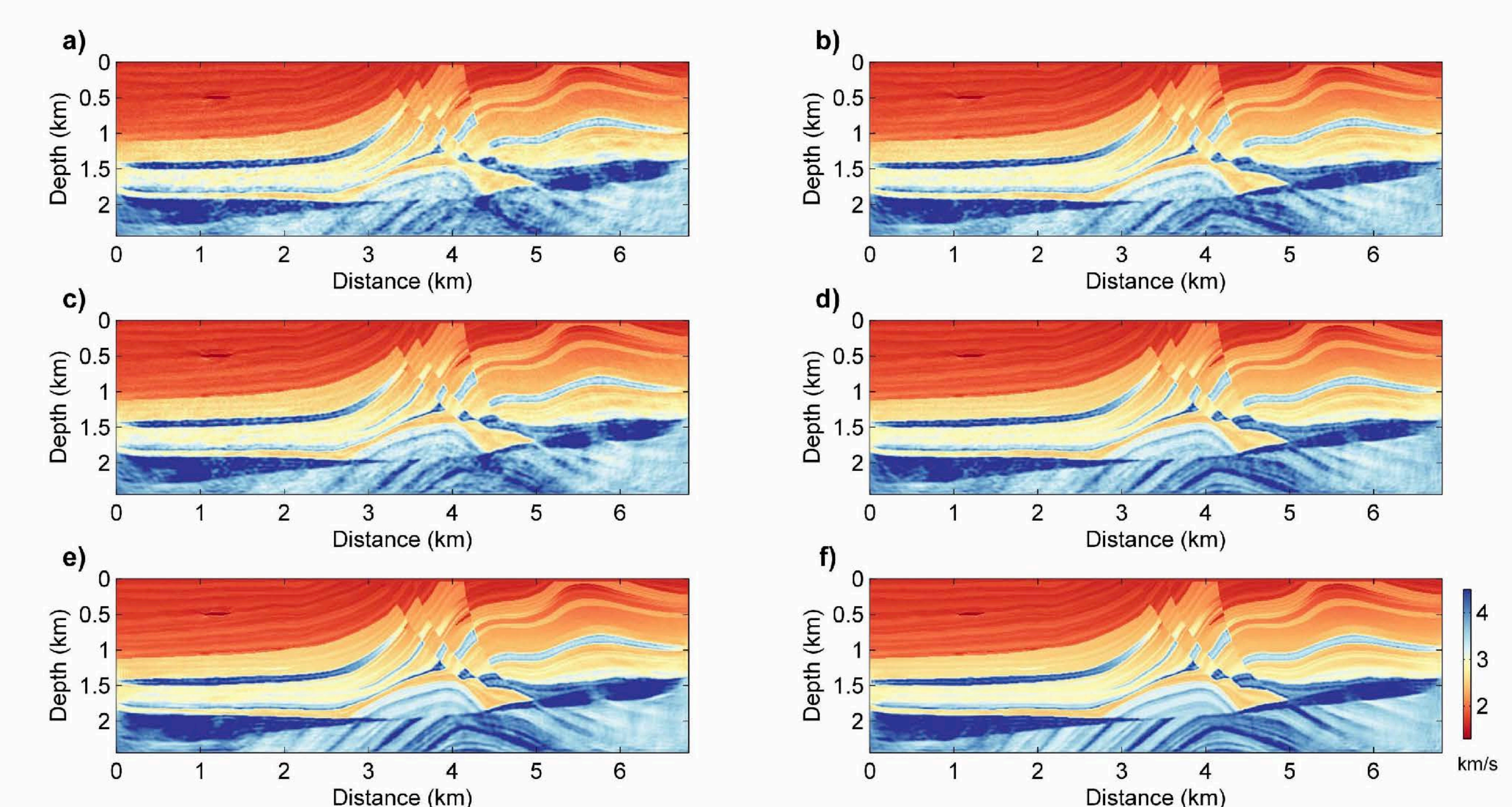


Figure 5. (a) Stacking $N_p=7$ (mono-frequency); (b) Stacking $N_p=7$ (overlap); (c) Stacking $N_p=11$ (mono-frequency); (d) Stacking $N_p=11$ (overlap); (e) SP (mono); (f) SP (overlap).

Acknowledgements

This research was supported by the Consortium for Research in Elastic Wave Exploration Seismology (CREWES).